A. Hassan, R. Künnemeyer, A. A. Dorrington, A. Payne, 'Proof of Concept of Diffuse Optical Tomography Using Time-of-Flight Range Imaging Cameras', *Proceedings of Electronics New Zealand Conference 2010*, pp. 115–120, Hamilton, New Zealand, November 2010.

Proof of Concept of Diffuse Optical Tomography Using Time-of-Flight Range Imaging Cameras

Ahmad Hassan, Rainer Künnemeyer, Adrian Dorrington, and Andrew Payne

School of Engineering, University of Waikato,
Private Bag 3105, Hamilton, New Zealand.
ash12@waikato.ac.nz.

Abstract: Diffuse optical tomography is an optical technique to create 3-dimensional images of the inside of highly scattering material. Research groups around the world have been developing imaging systems using various source-detector arrangements to determine optical properties of biological tissue with a focus on medical applications. In this paper we investigate whether a range imaging camera can be used as a detector array. We used time-of-flight range imaging cameras instead of the conventional source-detector array used by others. The results provided in this paper show reconstructed images of absorption and reduced scattering of an object submerged in a tissue simulating phantom. Using the ranging camera XZ422 Demonstrator and the NIRFAST software package, we reconstructed 2D images of a 6 mm metal rod submerged in the centre of a 5 cm deep tank filled with 1% Intralipid^{TM}. We have shown for the first time that range imaging cameras can replace the traditional detectors in diffuse optical tomography.

Keywords: Diffuse optical tomography, range imaging, NIRFAST

1 INTRODUCTION

Diffuse Optical Tomography (DOT) is a medical imaging techniques that has been under research and development since the early 1990s [1]. It is an alternative to current imaging techniques such as Magnetic Resonant Imagining (MRI) and X-ray computed tomography. DOT is non-invasive, non-ionising, low cost and also has an order of magnitude faster temporal resolution than that of (MRI) [2]. For example, DOT has the ability of producing information about the oxy-haemoglobin and deoxy-haemoglobin concentrations by measuring the optical properties (absorption and reduced scattering) of tissues, and hence it is being used in functional brain imaging and optical mammography [1-3].

There are three types of DOT measurement techniques: time domain, continuous wave domain and frequency domain [3, 4]. The time domain technique passes pulsed light through the area under test and measures the time delay between the incident and received pulse. The continuous wave technique measures only the attenuated light intensity passed through the tissue, whereas the frequency domain technique passes intensity modulated light through the area under test and measures both phase and intensity of the received modulated light relative to the incident [5].

Many research groups around the world have been developing DOT systems using different measurement techniques, source-detector arrangement and reconstruction algorithm. The frequency domain technique has become very popular over the recent years. The basic components needed are modulated light sources placed at various locations and discrete detectors which measure phase and intensity relative to the source modulation. In this research we present a proof of concept DOT system using time-of-flight 3D range imaging cameras and an open source reconstruction software (NIRFAST) [6] to detect and reconstruct images of objects submerged in tissue-simulating phantom.

2 BACKGROUND

2.1 Time-of-Flight Range Imaging

Time-of-flight range imaging is a technique used by several off-the-shelf camera modules such as those developed by Canesta Inc. (Sunnyvale, California, USA). Each of these camera modules work by illuminating a scene with a modulated light source, then measures the time it takes for the modulated light to reach an object and reflects back to the camera. The time delay is indi-

rectly determined by the phase shift created between the reflected and the incident modulated light. Knowing the speed of light c and the modulation frequency f_m (hence the modulation wavelength λ_m), and the phase shift φ, the distance d on each pixel can be calculated as [7]:

$$d = \frac{\varphi c}{4\pi f_m} = \frac{\varphi \lambda_m}{4\pi} \quad (1)$$

The intensity or active brightness can also be calculated for each pixel using Equation 2, where A_0, A_1, A_2, A_3 are pixel brightness values recorded at phase offsets of 0°, 90°, 180°, and 270° respectively.

$$Intensity = \frac{\sqrt{(A_0 - A_2)^2 + (A_1 - A_3)^2}}{2} \quad (2)$$

2.2 Optical Properties of Biological Tissues

2.2.1 Absorption and Scattering

When light travels in biological tissues it exhibits multiple scattering and absorption. Therefore, biological tissues are considered turbid media. These phenomena (absorption and scattering) occur due to the physical properties of the turbid medium. As light enters a turbid medium, it is scattered by particles, biological cells, or other discontinuities in refractive index. This diffusion causes the photons to take multiple paths. In addition, some photons are absorbed by molecules, causing the light to be attenuated as it propagates through the medium (Figure 1).

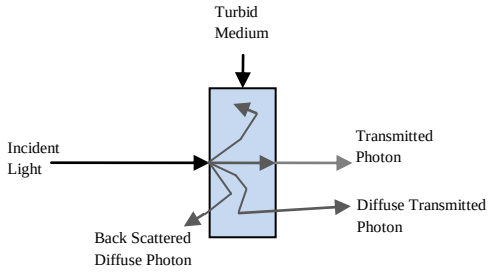

Figure 1: Light scattering and absorption in turbid medium.

Penetrating deep tissues is the main limitation in optical tomography due to the strong attenuation caused by absorption. However, absorption in the near-infrared region (between 610 to 910 nm) is orders of magnitude lower than in the visible spectrum [9, 10].

When a scattering medium is illuminated by a modulated light source, the light intensity and phase change with distance from the source. The slope of the amplitude of the AC component, I_{AC}, and the slope of the phase, ϕ, is given in Equation 3 and 4 [11].

$$I_{AC} = -\sqrt{\frac{3}{2}\mu_a(\mu_a + \mu_s')}\left[\sqrt{1+\left(\frac{\omega}{\upsilon\mu_a}\right)^2} + 1\right]^{\frac{1}{2}} \quad (3)$$

$$\phi = \sqrt{\frac{3}{2}\mu_a(\mu_a + \mu_s')}\left[\sqrt{1+\left(\frac{\omega}{\upsilon\mu_a}\right)^2} - 1\right]^{\frac{1}{2}} \quad (4)$$

where ω is the angular frequency of the modulation, υ the speed of light in the medium, μ_a the absorption, and μ'_s the reduced scattering coefficient.

When the slopes of AC intensity and phase are known, the equations can be solved for the absorption and scattering properties of the turbid medium.

2.2.2 Tissue-Simulating Phantom

Tissue-simulating phantoms are materials used in optics research labs. They exist in solid and liquid forms. Intralipid™ is a commercially available milky solution with concentration 10%, 20% and 30%. It contains Soybean oil, Lecithin, Glycerine and water, and it is normally used in hospitals to feed weak patients. It is also used to simulate body tissue when conducting experiments. The absorption coefficient of Intralipid™ at 1% concentration is very similar to water and ranges from 0.02 cm^{-1} to 0.3 cm^{-1}. However, the scattering coefficient is approximately constant (10 cm^{-1}) over the near-infrared wavelength range [11].

3 METHOD

In this study a 6 mm metal rod was submerged in a transparent plastic tank filled with 1% Intralipid™. A range imaging camera was placed facing one end of the tank, and a laser beam was shone on the other side.

3.1 Hardware Setup

The hardware setup shown in figure 2 consists of:

- Range imaging camera (XZ422 Demonstrator) made by Canesta Inc. (Sunnyvale, California, USA) with image resolution of 160×120.
- Near-infrared laser, 850 nm, with an average output power of 50 mW. The laser beam was focused to a 3mm spot on the target.
- Clear plastic tank made out of acrylic sheet filled with tissue-simulating phantom (1% Intralipid™).

- 6 mm diameter metal rod submerged in the tank.

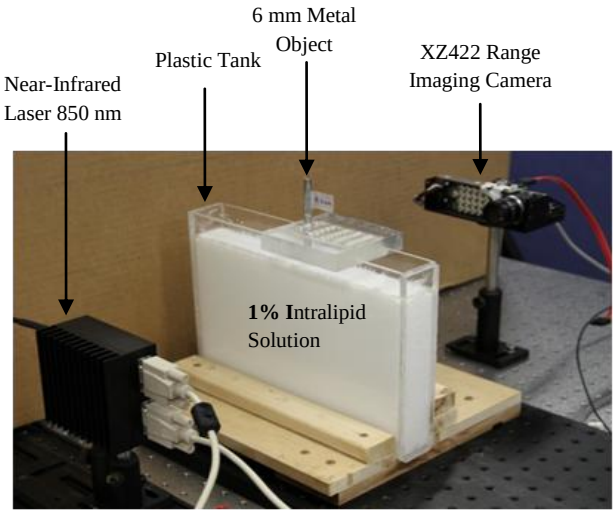

Figure 2: Hardware setup.

The laser beam is collimated and shone onto the tank from one end. Light will then diffuse as it enters the tank. Some of the light propagates through to the other side of the tank. These transmitted photons are captured by the camera and ultimately carry phase and intensity information about the submerged object.

3.2 Processing and Reconstruction

MATLAB™ was used for processing the data produced by the camera (active brightness and range). However, image reconstruction is done using NIRFAST (Near-Infrared Florescence and Spectral Tomography) [6]. NIRFAST is a software package which simulates light propagation in biological tissues based on the finite element method. It can process single wavelength absorption and reduced scattering, multi-wavelength and also fluorescence models [6]. In this study we only used the 2D standard single wavelength absorption and reduced scattering image reconstruction tool. Hence, we used a 2D mesh to simulate a horizontal slice of our tank as shown in figure 3.

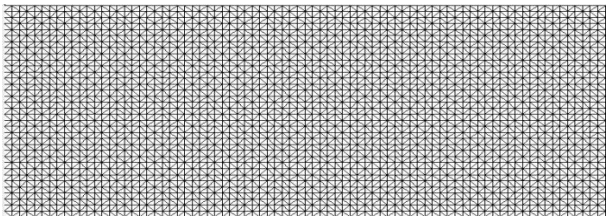

Figure 3: 2D mesh created by NIRFAST

Four experiments were repeated using one, five, seven and twenty-one sources with 6 mm spacing, keeping the number of detectors fixed (twenty-one detectors). The detectors were configured on the range image by choosing pixels across the captured images.

The sources are turned on one after the other and data is recorded for a set of detectors. For the three cases (one-source, five-sources and seven-sources) the data is obtained from all the 21-detectors. In contrast, the data collected from the 21-sources were obtained from only 14-detectors (Figure 4).

(a)

Case 1, 5 and 7 sources, all the detectors are used by all the sources

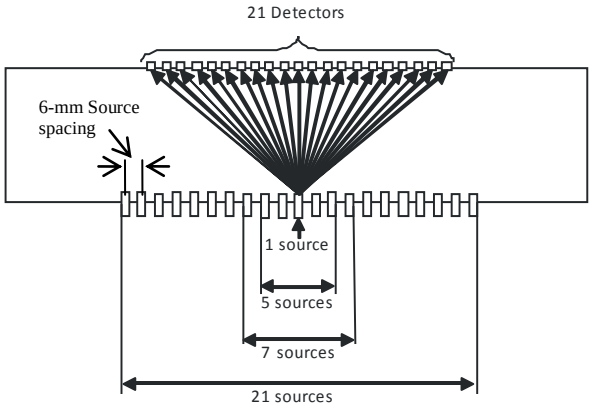

(b)

Case 21-sources, only 14-detectors are used by all the 21-sources

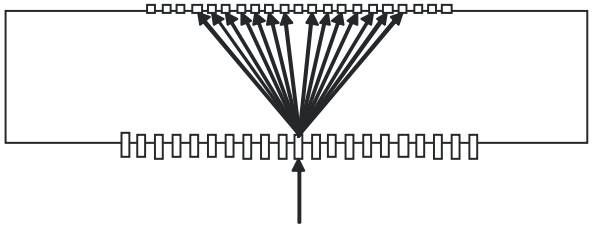

Figure 4: Source-detector configuration, (a) in case 1, 5 and 7 sources, (b) in case 21 sources.

3.3 Calibration

The software was used to generate simulated results of phase and intensity. These results were then compared with the results produced by our range imaging camera. Due to phase delay in the camera electronics, the software and the camera have different scales, therefore, the phase and intensity data produced by the camera had to be fitted to match the software data. This was really important because one of the software requirements in reconstructing images of absorption and reduced scattering is the phase and intensity data obtained from the camera. This data fitting process was achieved by the polynomial fitting tool box available in MATLAB™.

4 RESULTS AND DISCUSSION

4.1 Calibration

Figure 5 shows a plot of phase and intensity obtained from the camera and NIRFAST [6]. Clearly, there is an offset between the camera and NIRFAST scales. This issue was resolved by using a secound degree polynomial function to fit the data as shown in figures 6 and 7. The result is shown in figure 8, where the camera and software functions are fitted nicely.

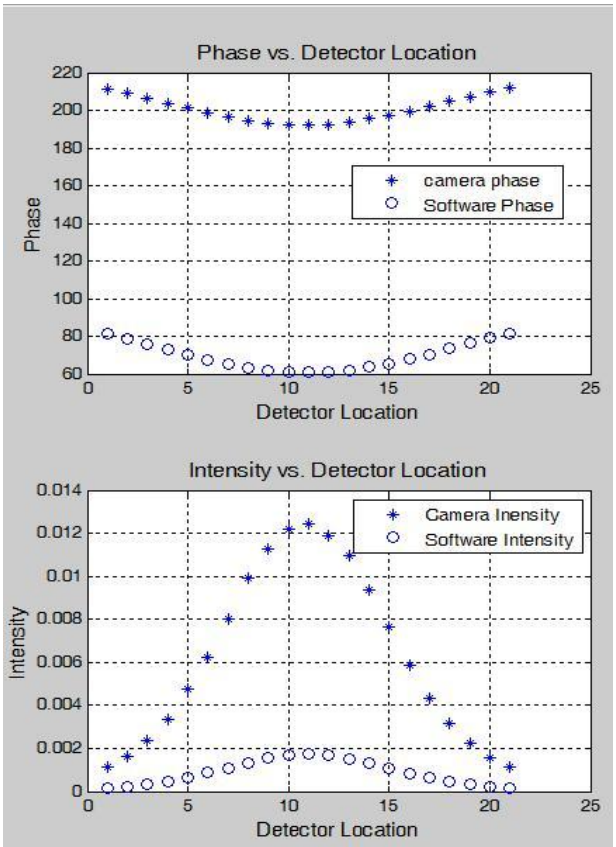

Figure 5: Un-calibrated phase and Intensity functions.

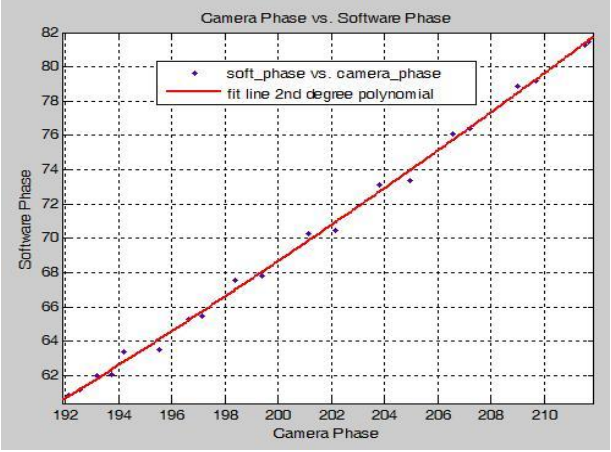

Figure 6: 2nd degree poly-fit of phase function.

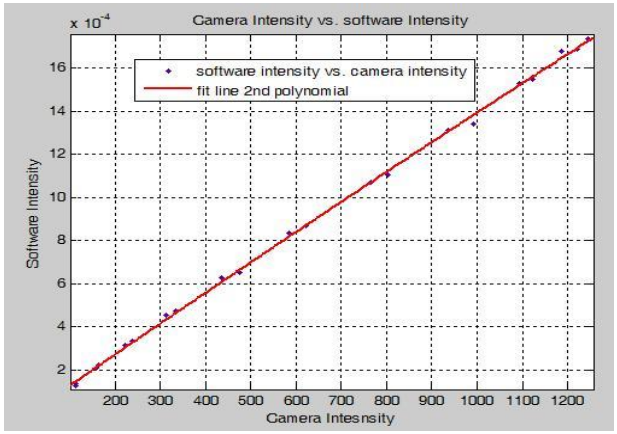

Figure 7: 2nd degree poly-fit of intensity function.

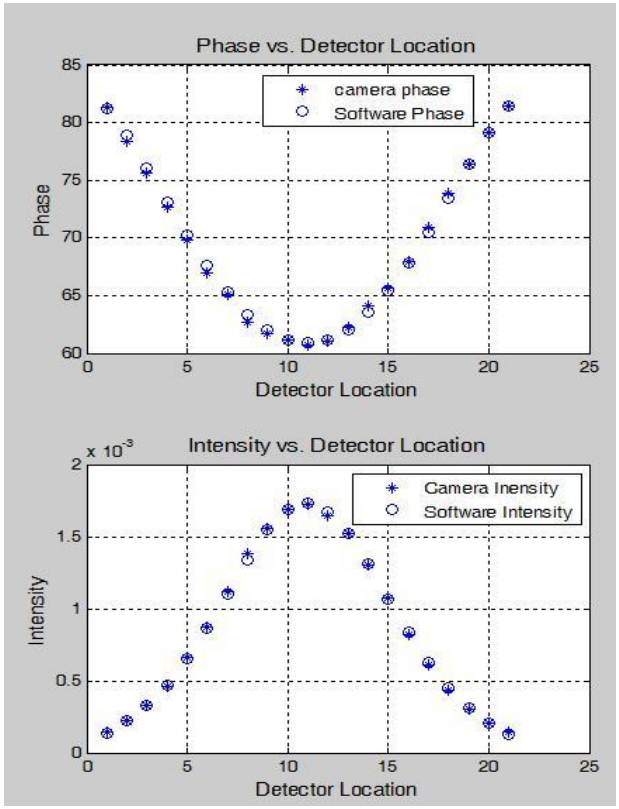

Figure 8: Calibrated phase and intensity functions.

4.2 Reconstruction Results

Figure 9 showns a photographic image of the location of the object. Figure 10, in contrast, shows a sequence of reconstructed images with different number of sources. The reduced scatering images μ_s show almost no evidence of the object as it is considered a black object when submerged in the tank, and therefore no scattering has occurred. However, the absorption images μ_a show an outline of the object in all the cases, but the reconstructed image (figure 10d) is the closest estimation of object's size and location when compared with the real image (figure 9).

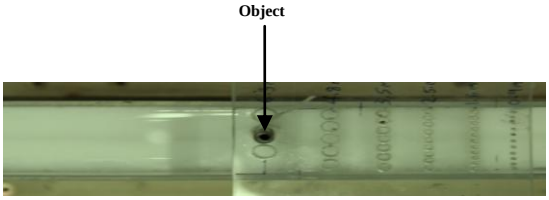

Figure 9: Photographic image (top view) of the tank with the object submerged.

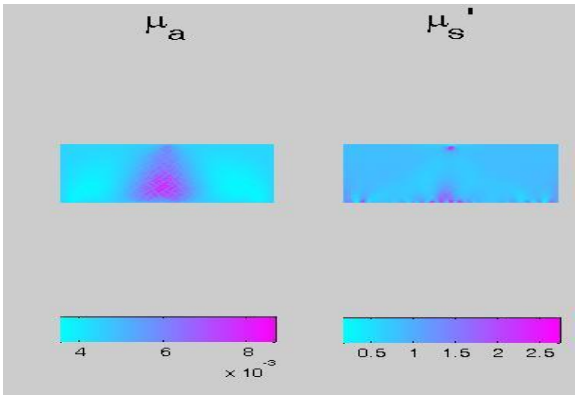

a)

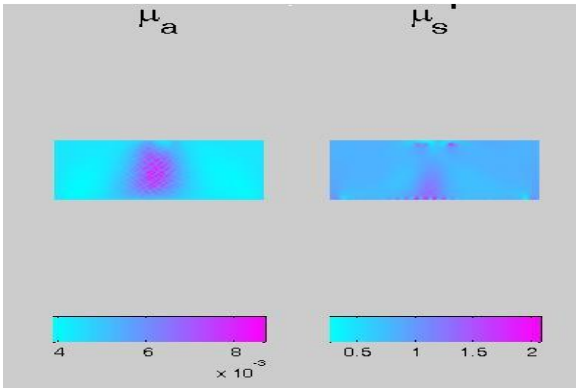

b)

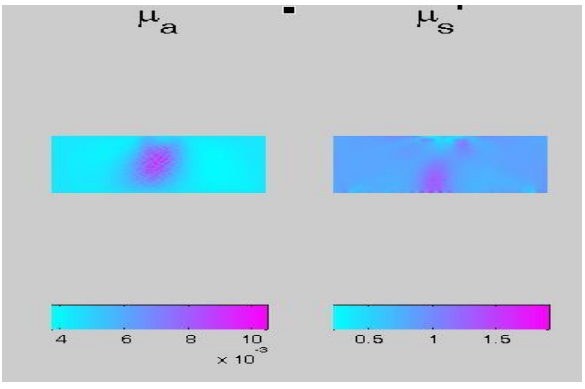

c)

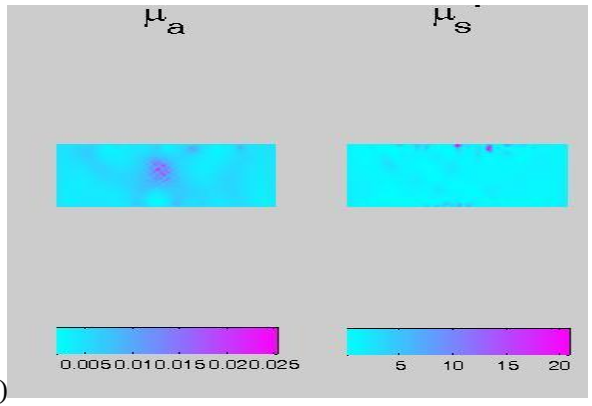

d)

Figure 10: Reconstructed images of absorption, μ_a, and reduced scattering, μ_s (a) with a single source (b) with 5 sources (c) with 7 sources (d) with 21 sources.

These results indicate that increasing the number of sources will improve the reconstructed image, i.e., more information is obtained about the object from multiple angles as shown in figure 11. However, the source location has not been optimised in this work, and will be considered in future work.

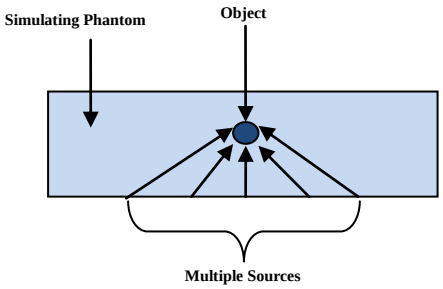

Figure 11: Top view model showing how light is obtaining spatial information about the object.

5 FURTHER WORK

In this study it was found that diffuse optical tomography is possible using 3D range imaging technology. However, more research is required to characterize this imaging system. The results highlighted that multiple sources are required to perform diffuse optical tomography. The optimum number of sources is yet to be determined with further experiments. Furthermore, NIRFAST incorporates 3D meshes which potentially can be used to reconstruct 3D images of tissue optical properties.

6 CONCLUSIONS

We have demonstrated experimentally as proof of concept the practicality of using time-of-flight range imaging cameras for non-contact signal detection in DOT medical imaging. Reconstructed images of absorption and reduced scattering are presented in this research. These results show that multiple sources are required to obtain spatial information of objects submerged in a simulating phantom. Although further investigation is needed, this could be the starting point to further develop the current set up to a fully integrated diffuse optical tomography system.

7 REFERENCES

[1] D. Piao, H. Dehghani, S. Jiang, S. Srinivasan, and B. W. Pogue, "Instrumentation for video-rate near-infrared diffuse optical tomography," *Review of Scientific Instruments*, vol. 76, pp. 1-13, 2005.

[2] N. Cao and A. Nehorai, "Tumor localization using diffuse optical tomography and linearly constrained minimum variance beamforming," *Opt. Express*, vol. 15, pp. 896-909, 2007.

[3] A. Corlu, R. Choe, T. Durduran, K. Lee, M. Schweiger, S. R. Arridge, E. M. C. Hillman, and A. G. Yodh, "Diffuse optical tomography with spectral constraints and wavelength optimization," *Appl. Opt.*, vol. 44, pp. 2082-2093, 2005.

[4] C. Li, S. R. Grobmyer, L. Chen, Q. Zhang, L. L. Fajardo, and H. Jiang, "Multispectral diffuse optical tomography with absorption and scattering spectral constraints," *Appl. Opt.*, vol. 46, pp. 8229-8236, 2007.

[5] S. J. Erickson and A. Godavarty, "Hand-held based near-infrared optical imaging devices: A review," *Medical Engineering and Physics*, vol. 31, pp. 495-509, 2009.

[6] H. Dehghani, M. E. Eames, P. K. Yalavarthy, S. C. Davis, S. Srinivasan, C. M. Carpenter, B. W. Pogue, and K. D. Paulsen, "Near infrared optical tomography using NIRFAST: algorithm for numerical model and image reconstruction," *Communications in Numerical Methods in Engineering*, vol. 25, pp. 711-32, 2009.

[7] A. A. Dorrington, M. J. Cree, A. D. Payne, R. M. Conroy, and D. A. Carnegie, "Achieving sub-millimetre precision with a solid-state full-field heterodyning range imaging camera," *Measurement Science and Technology*, vol. 18, pp. 2809-2816, 2007.

[8] A. A. Dorrington, C. D. B. Kelly, S. H. McClure, A. D. Payne, and M. J. Cree, "Advantages of 3D time-of-flight range imaging cameras in machine vision applications," in *Proceeding of the 16th Electronics New Zealand Conference (ENZCon), Dunedin, New Zealand*, Dunedin, New Zealand, 18-20 November, 2009, pp. 95-99.

[9] C. Balas, "Review of biomedical optical imaging-a powerful, non-invasive, non-ionizing technology for improving in vivo diagnosis," *Measurement Science & Technology*, vol. 20, p. 104020 (12 pp.), 2009.

[10] B. W. Pogue, S. C. Davis, S. Xiaomei, B. A. Brooksby, H. Dehghani, and K. D. Paulsen, "Image analysis methods for diffuse optical tomography," *Journal of Biomedical Optics*, vol. 11, pp. 33001-1, 2006.

[11] B. Cletus, 2010, "Wavelength Tuneable Frequency Domain Photon Migration Spectrometer for Tissue-like Media", PhD thesis, University of Waikato, Hamilton, New Zealand.